Research, Society and Development, v. 10, n. 7, e57510716920, 2021
(CC BY 4.0) | ISSN 2525-3409 | DOI: http://dx.doi.org/10.33448/rsd-v10i7.16920

Y-PSZ/Bioglass 45S5 composite obtained by the infiltration technique of porous pre-sintered bodies using sacrificial molding

Compósito Y-PSZ/Biovidro 45S5 obtido pela técnica de infiltração de corpos porosos pré-sinterizados utilizando moldagem de sacrifício

Composite Y-PSZ / Bioglass 45S5 obtenido mediante la técnica de infiltración de cuerpos porosos presinterizados mediante moldeo de sacrifício

Received: 06/07/2021 | Reviewed: 06/15/2021 | Accept: 06/15/2021 | Published: 06/25/2021

Raphael de Oliveira Luzo
ORCID: https://orcid.org/0000-0003-4041-6337
State University of Rio de Janeiro, Brazil
E-mail: rapha.luzo@gmail.com
Vinícios Dias de Oliveira
ORCID: https://orcid.org/0000-0003-2914-0317
State University of Rio de Janeiro, Brazil
E-mail: vinicios.dias@hotmail.com
Marco Antonio da Costa
ORCID: https://orcid.org/0000-0001-6077-9181
Volta Redonda University Center, Brazil
E-mail: marco.costa9384@gmail.com
Claudinei dos Santos
ORCID: https://orcid.org/0000-0002-9398-0639
State University of Rio de Janeiro, Brazil
E-mail: claudinei@pesquisador.cnpq.br
José Eduardo Vasconcellos Amarante
ORCID: https://orcid.org/0000-0002-6796-8265
Fluminense Federal University, Brazil
E-mail: jeduardo@id.uff.br
Juliana Kelmy Macário Barboza Daguano
ORCID: https://orcid.org/0000-0001-6098-6826
Renato Archer Information Technology Center, Brazil
E-mail: juliana.daguano@cti.gov.br
Kurt Strecker
ORCID: https://orcid.org/0000-0001-6164-7906
Federal University of São João del-Rei, Brazil
E-mail: strecker@ufsj.edu.br
Manuel Fellipe Rodrigues Pais Alves
ORCID: https://orcid.org/0000-0001-7671-5684
State University of Rio de Janeiro, Brazil
E-mail: manuelfellipealves@gmail.com

Abstract
The aim of this work was to obtain porous ceramic parts based on Zirconia stabilized with 5mol.% Yttria (5Y-PSZ), suitable for the infiltration with bioactive glasses, using 3D printed sacrificial polymeric molds. In a first step, honeycomb structured molds were designed with the SolidWorks® software and manufactured by 3D printing using polylactic acid filaments (PLA). These molds were filled with a ceramic mass composed of 5Y-PSZ nanoparticles containing 3wt% polymeric binder and consolidated under pressure of 10MPa and then sintered at 1200 °C-30 min the polymeric molds were consumed. The obtained hexagonal-shaped, porous 5Y-TZP bodies were infiltrated with the bioactive glass 45S5, calcium sodium phosphosilicate, at 1350 °C. The materials were characterized by their relative density, their phase composition by X-ray diffraction analysis, and their microstructure by scanning electron microscopy (SEM-EDS), besides their mechanical properties of hardness and fracture toughness. Pre-sintered 5Y-PSZ substrates exhibit relative density around 75%, and 90% after sintering and Bioglass infiltration. The samples' microstructure is composed of a 5Y-PSZ matrix of sub-micrometric zirconia grains with an average size of 1.0 μm, besides the secondary infiltrated glassy phase homogeneously distributed, with a Ca/P ratio of 1.7, close to the ideal proportion for hydroxyapatite formation. In conclusion, sacrificial molding is an interesting route to obtaining dense Y-PSZ/Bioglass 45S5 composite in a honeycomb format.
Keywords: Composite; 5Y-PSZ; Bioglass 45S5; 3D printing; Infiltration; Characterizations.

Resumo

O objetivo deste trabalho foi a obtenção de peças cerâmicas porosas à base de Zircônia estabilizada com 5mol.% de ítria (5Y-PSZ), adequadas para a infiltração com vidros bioativos, utilizando moldes poliméricos sacrificiais impressos em 3D. Em uma primeira etapa, os moldes estruturados em honeycombs foram projetados com o software SolidWorks® e fabricados por impressão 3D usando filamentos de ácido polilático (PLA). Esses moldes foram preenchidos com uma massa cerâmica composta por nanopartículas 5Y-PSZ contendo 3% em peso de ligante polimérico e consolidados sob pressão de 10MPa e então sinterizados a 1200 ° C-30 min os moldes poliméricos foram consumidos. Os corpos 5Y-TZP porosos de forma hexagonal obtidos foram infiltrados com o vidro bioativo 45S5, fosfosilicato de cálcio e sódio, a 1350 ° C. Os materiais foram caracterizados quanto à densidade relativa, composição de fases por difração de raios X e microestrutura por microscopia eletrônica de varredura (MEV-EDS), além de propriedades mecânicas de dureza e tenacidade à fratura. Substratos pré-sinterizados 5Y-PSZ exibem densidade relativa em torno de 75% e 90% após sinterização e infiltração de Biovidro. A microestrutura das amostras é composta por uma matriz 5Y-PSZ de grãos de zircônia submicrométricos com tamanho médio de 1,0 μm, além do infiltrado secundário fase vítrea distribuída homogeneamente, com relação Ca / P de 1,7, próxima à proporção ideal para formação de hidroxiapatita. Em conclusão, a moldagem sacrificial é uma rota interessante para a obtenção de compósito Y-PSZ / Bioglass 45S5 denso em formato de colmeia.

Palavras-chave: Compósito; 5Y-PSZ; Bioglass 45S5; Impressão 3D; Infiltração; Caracterizações.

Resumen

El objetivo de este trabajo fue obtener piezas cerámicas porosas a base de Zirconia estabilizada con 5mol.% Yttria (5Y-PSZ), aptas para la infiltración con vidrios bioactivos, utilizando moldes poliméricos de sacrificio impresos en 3D. En un primer paso, se diseñaron moldes con estructura de panal con el software SolidWorks® y se fabricaron mediante impresión 3D utilizando filamentos de ácido poliláctico (PLA). Estos moldes se llenaron con una masa cerámica compuesta de nanopartículas de 5Y-PSZ que contenían un 3% en peso de aglutinante polimérico y se consolidaron a una presión de 10 MPa y luego se sinterizaron a 1200ºC-30 min. Se consumieron los moldes poliméricos. Los cuerpos de 5Y-TZP porosos de forma hexagonal obtenidos se infiltraron con el vidrio bioactivo 45S5, fosfosilicato de calcio y sodio, a 1350 °C. Los materiales se caracterizaron por su densidad relativa, su composición de fases por análisis de difracción de rayos X y su microestructura por microscopía electrónica de barrido (SEM-EDS), además de sus propiedades mecánicas de dureza y tenacidad a la fractura. Los sustratos presinterizados de 5Y-PSZ exhiben una densidad relativa de alrededor del 75% y el 90% después de la sinterización y la infiltración de Bioglass. La microestructura de las muestras está compuesta por una matriz 5Y-PSZ de granos de circonio submicrométrico con un tamaño promedio de 1.0 μm, además de la fase vítrea infiltrada secundaria distribuida homogéneamente, con una relación Ca / P de 1.7, cercana a la proporción ideal para formación de hidroxiapatita. En conclusión, el moldeo de sacrificio es una ruta interesante para obtener un compuesto denso Y-PSZ / Bioglass 45S5 en un formato de panal.

Palabras clave: Composite; 5Y-PSZ; Bioglass 45S5; Impresión 3D; Infiltración; Caracterizaciones.

1. Introduction

With increasing lifespan, human organs and body tissues tend to decline their functioning and, therefore, materials compatible with the human body are developed by the so-called tissue engineering to repair or replace human´s natural materials or organs, such as bone, cartilage, blood vessels, etc. Biomaterials are substances that can be used to replace human organs or tissues to maintain certain body functions of an individual. The basic requirement for a biomaterial is its compatibility with the human body environment, i.e., it doesn´t cause undesirable or inappropriate effects for the organism (Hench, 1991) (Jones et. al., 2016) (Juraski et. al. 2021).

Three main classes of biomaterials can be distinguished: (1) bio-inert materials, which are incapable of inducing any biological interfacial link between the implant and the host tissue; (2) bio-active materials which may interact with body tissues, favoring processes such as the fixation of implants and regeneration of tissues and (3) bio-resorbable materials which are gradually absorbed by the body and are replaced by new tissue *in vivo* (Kim et al., 2021) (Campana et. al., 2014).

In this context, the development of new materials, specifically of biocompatible composites, is of high importance in tissue engineering, especially in the area of bioceramics and biopolymers ((Hench, 1991). Composites are formed by the union of different materials, resulting in a new material with unique properties, or a combination of properties that starting compounds cannot achieve. These materials can induce processes which regenerate body tissue by the transport of cell populations and therapeutic agents, providing a structural support with mechanical properties similar to the human bone.

Biomaterials should ideally allow the growth of new tissues at the implantation site. Among these materials, hydroxyapatite (HA) $Ca_{10}(PO_{4)6}(OH)_2$ stands out as a bioactive ceramic with characteristics and composition similar to human bone. It can replace damaged hard tissues, repair bone defects in maxillofacial reconstruction and orthopedic surgeries. The combination of calcium phosphate phases creating porous biphasic compounds results in a higher reactivity of these ceramics and with faster responses when exposed to the physiological medium (Baino & Fiune 2018). Bioactive glasses with a composition close to HA, such as the Bioglass 45S5®, calcium sodium phosphosilicate, (Baino et. al. 2019) are excellent candidates for the manufacture of implantable biomaterials due to their versatility and exceptional ability to stimulate osseointegration and osteogenesis through release of ions by dissolution (mainly silicate and Ca^{2+} ions) promoting bone cell responses towards regeneration and self-repair (Rahaman et. al., 2011) (Hoppe et. al. 2011) (Baino et. al., 2018). However, its low mechanical resistance impairs its application as a monolithic biomaterial. In this context, the union of the biological properties of these glasses with bioinert ceramics of high mechanical resistance, such as zirconia ceramics (Reveron & Chevalier, 2021) is an attractive alternative, aiming at structural applications of medium mechanical demand.

The use of prototypes obtained by 3D printing is considered of great importance within the manufacturing processes of new prototypes due to the speed of production, the associated low cost, and the reduction of the time spent in the analysis of the viability of a new product developed by a new manufacturing route (Agarwala et. al., 1996) (Gibson et. al., 2010) (Karakurt et. al., 2020) (Zhou et. al., 2004). Implants of complex geometry are often required to treat some specific trauma. Furthermore, the surface characteristics of these parts, such as roughness, degradation rate, or bioactivity are also important. In this context, the sacrificial molding process may contribute to an optimized fabrication of bioceramic parts with controlled surface characteristics.

Thus, the aim of this work was the creation of sacrifice molds by 3D printing, filling them with a ceramic mass based on partially stabilized zirconia powder, and promoting the infiltration of the substrates with a considerable amount of Bioglass, to obtain dense materials with the favorable biological response.

2. Experimental Procedure

2.1 Materials

In this work, a nanoparticulate zirconia powder stabilized with 5 mol% Yttria, ZrO_2-Y_2O_3, TOSOH-Smile (Japan), with a particle size of 90 nm and containing 3wt.% polymer binder, was used to fabricate the ceramic substrates. These materials present high hydrothermal degradation resistance (Camposilvan et. al., 2018) comparing with traditional 3Y-TZP tetragonal zirconia ceramics (Guo & He, 2003). The glass used for the substrates' infiltration was a bioactive glass named as Bioglass 45S5 (Baino &Fiune 2019), whose processing details are described below.

2.2 Processing

2.2.1 Glass synthesis

Bioactive glass (45 SiO_2–24.5 CaO - 24.5 Na_2O – 6 P_2O_5 in wt.%) was produced by melting reagents (analytical grade powders of SiO_2, $CaCO_3$, Na_2CO_3, and $Ca_3(PO_4)_2$, Sigma - Aldrich) in a platinum crucible at 1500 °C, for 1h in air, using a heating rate of 5 °C/min. The molten material was quenched in deionized water to obtain a frit, which was ground using a mill with jars and spheres of alumina and passing through a 400 mesh sieve.

2.2.2 Fabrication of sacrifice molds by 3D printing.

The molds in the form of hexagonal colonies (Figure 1) with an internal wall thickness of 0.75 mm were designed using the SolidWorks® software. Then, the drawing in a "* stl" file was inserted into the CURA® software. The 3D printing of the

molds was performed on a Tevo Tarantula Pro printer, using polymeric filaments based on 3DFILA polylactic acid (PLA) with a nominal diameter of 1.75 mm (density: 1.04 g/cm³; melting temperature: 200 – 230 °C) and the following print parameters: 0.2 mm Layer Height, Number of Upper and Lower Layers = 1, Fill Orientation: Honeycomb, Extrusion Temperature: 170 ºC, Table Temperature: 50 ºC, Cooler Speed: 100% and Print Speed: 30 mm/s.

Figure 1 – Drawing created in SolidWorks software (a) and polymeric molds fabricated by 3D printing (b and c).

(a) (b) (c)

Source: Authors.

2.2.3 Fabrication of Bioglass infiltrated Y-PSZ composites

A paste of the zirconia ceramic powder containing binder was prepared by adding isopropyl alcohol. The printed molds with hexagonal colonies were filled with this paste, as shown in Figure 2. Then, its metallic base of tempered steel with approximately 5 kgf was positioned on top of the mold to carry out a pre-compaction.

Figure 2 - a) Filling the mold with the ceramic powder, b) accommodation and application of isopropyl alcohol, c) completion of the molding step, and d) 5Y-PSZ substrates after firing and removal of the sacrificial polymeric mold.

(a) (b) (c)

d)

Source: Authors.

The compacted samples were heat-treated in an F1350-MAITEC oven, aiming to consolidate the cells and extract the polymer present in the mold. The cycle was: heating up to 350 °C, with a heating rate of 1 °C/min and holding for 120 minutes, heating up between 350 °C and 1200 °C (5 °C/min) and holding also for 120 minutes, followed by a controlled cooling at a rate of 10°C/min. The relative densities of the porous 5Y-PSZ cells (substrates) were determined geometrically.

The Bioglass powder was mixed with polyethylene glycol (Mn = 400 g/mol), and a thick layer of this paste was put onto the surface of the 5Y-PSZ colonies, as shown in Figure 3. Then, the glass paste was left to rest for 60 min, and later the samples were subjected to densification/infiltration using the following cycle: * Tamb. - 150 °C (5 °C/min) 30 minutes; * 150 - 1100 °C (3 °C/min) 60 minutes; * 1100 - 1350 °C (1 °C/min) 60 minutes; * 1350 °C - Also 2 °C / min. Comparatively, 5Y-PSZ substrates without infiltrated Bioglass were also densified under the same conditions.

Figure 3 - a) preparation of the Bioglass 45S5 paste; b) deposition of the Bioglass paste on the surface of the 5Y-PSZ pre-sintered ceramics.

(a)

(b)

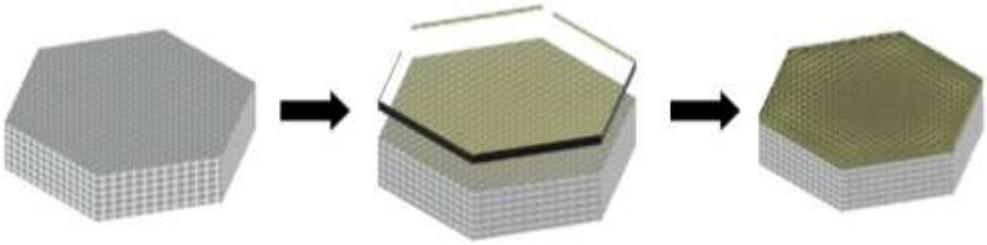

porous 5Y-PSZ subtract

deposition of Bioglass paste on the 5Y-PSZ subtracts

Bioglass infiltration of the porous subtract and shrinkage

Source: Authors.

2.3 Characterization

After sintering (infiltration), densification was evaluated by their density measured using the immersion method based on Archimedes principle, with a precision scale Discovery Ohaus, following ASTM C373-88 standard.

Phase analysis of the starting powders and the sintered samples was carried out by X-ray diffraction (Panalytical Empyrean Diffractometer, Cu-Kα radiation, λ = 0,15443nm, 45 kV), step size = 0.05° and of 5s exposure per position. The phases were identified by comparison with the JCPDS file, using the program Match! 2, Crystal impact.

The starting powder and sintered samples were observed by scanning electron microscopy (JEOL 7100FT) with a coupled EDS detector (Oxford X-Max 80 mm^2). For the microstructural evaluation, polished and original surfaces were analyzed.

The polished surfaces of monolithic 5Y-TZP samples were thermally etched at 1350 °C-15 min, and a thin layer of gold was deposited using K550X (Quorum Technologies-UK) metallizer, with a current of 30 mA for 2 minutes. The SEM micrographs were processed using an image analyzer. The grain size distribution was obtained considering the Feret diameter, at least 500 grains were measured.

Vickers hardness was measured by the indentation method (ASTM C1327-15) using a Vickers microhardness tester (Model TIME F100, China) with a load of 500 gF applied for 30 seconds. Twenty indentations were applied on each sample, considering cross-section of the infiltrated or sintered samples. The fracture toughness was calculated according to Equation (1):

$$K_{IC} = 0.016 \left(\frac{E}{H_V}\right)^{1/2} . \frac{L}{C^{3/2}} \quad (1)$$

where: K_{IC} = fracture toughness [MPa.m$^{1/2}$], E = modulus of elasticity [GPa], HV = Vickers hardness [GPa], L = indentation load [MN], C = average crack length [m].

3. Results and Discussions

3.1 Characterization of raw materials

Figure 4 shows an SEM micrograph and the X-ray diffraction pattern of the zirconia powder used in this work. According to manufacturing, this powder exhibits an average particle size of 90 nm, is sintered usually at a temperature around 1500 °C and is bioinert. Furthermore, to facilitate compaction, the powder contains about 5% of polymer binder. It is possible to observe that spherical agglomerates are formed due to the polymer binder added during its manufacture by spray-drying. The XRD diffractogram indicates that the powder is composed of monoclinic and tetragonal+cubic ZrO_2 as crystalline phases. The tetragonal+cubic ZrO_2 phase content is approximately 38%, while the monoclinic phase content is about 62%.

Figure 5 presents characterization results of the Bioglass powder. From the SEM micrograph (Fig 5 (a)), particles smaller than 80 µm and irregular shapes, typical of a brittle material, are identified. The X-ray diffraction pattern (Fig 5 (b)) shows an amorphous material profile with some defined crystallization peaks. Furthermore, Figure 5(c) presents chemical analysis by EDS, where the presence and distribution of Si, Na, Ca, and P, in addition to O, can be observed. Ca and P are the main components of hydroxyapatite, and a stoichiometric ratio of 1.71 enables the formation of tissues similar to human bone (Daguano et. al. 2013), depending on the controlled degradation time.

Figure 4 - a) SEM micrograph and b) X-ray diffraction of the Zirconia starting powder.

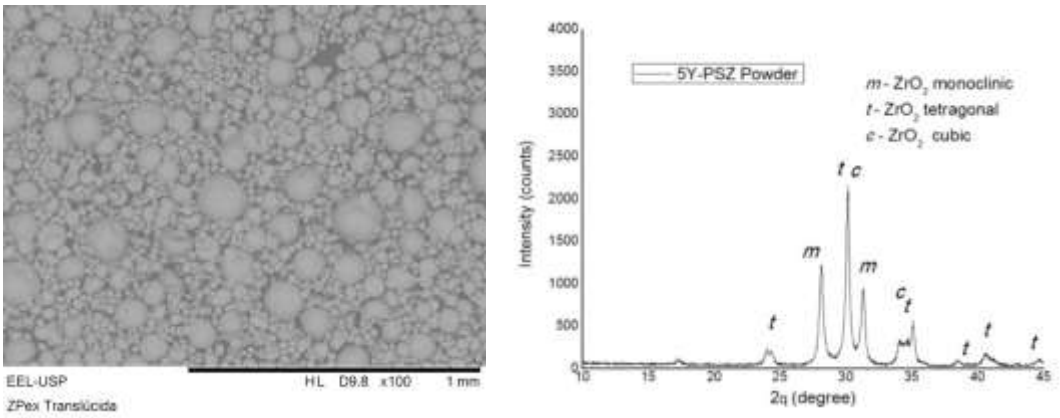

(a) (b)

Source: Authors.

Figure 5 - a) SEM and b) X-ray diffraction pattern of the bioglass powder.; c) EDS chemical analysis of Bioglass particles.

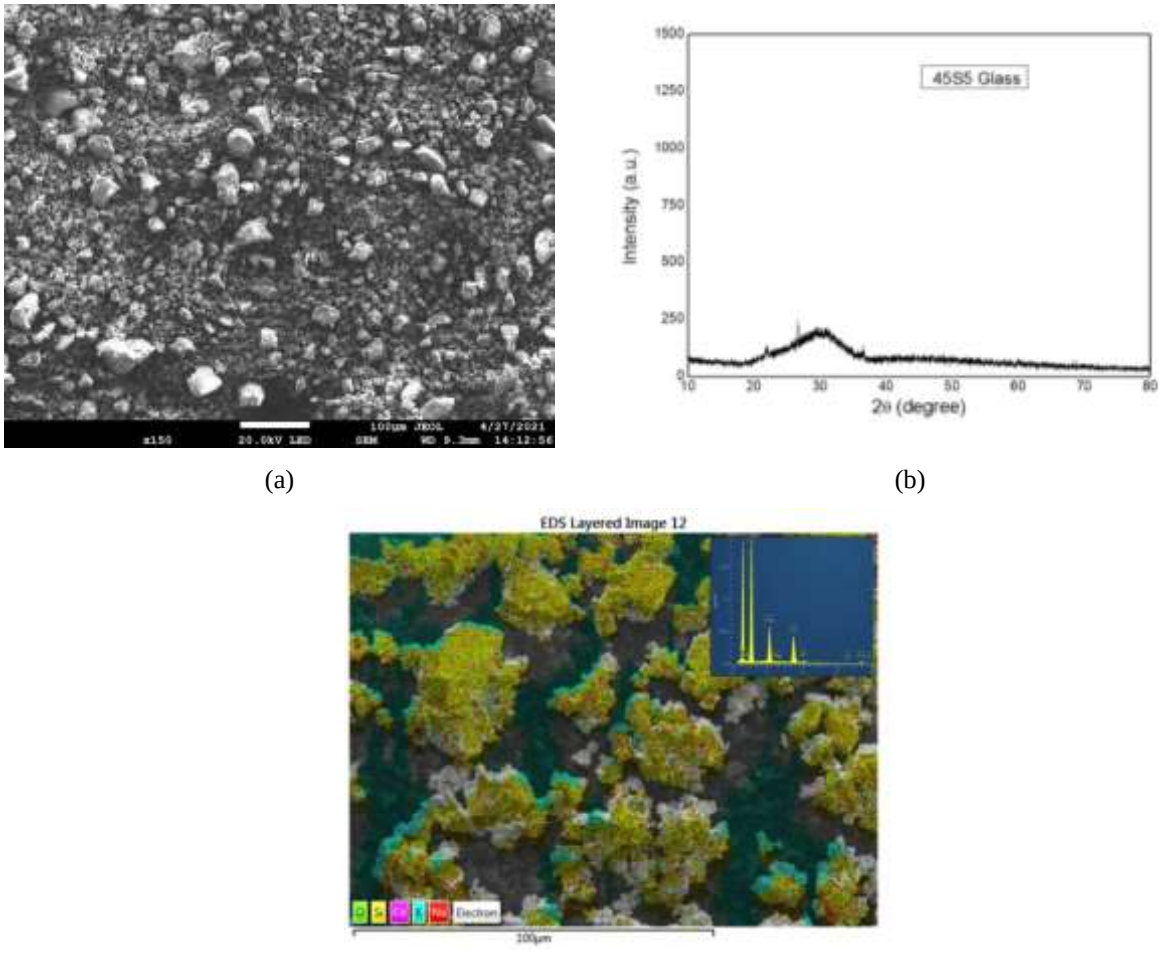

(a) (b)

(c)

Source: Authors.

3.2 Characterization of sintered bodies

The pre-sintering process at 1200 ºC resulted in Zirconia hexagonal ceramic cells with a relative density close to 73-75% of the theoretical density. In general, the samples maintained the original geometry of the mold created by 3D printing, see

Figure 6. The PLA mold evaporates during firing in a small temperature range between 330 - 395ºC and preferably evaporates through the interconnected pores of the ceramic matrix, without leaving residues remaining on the ceramic substrate. After the pre-sintering process, having eliminated the polymer sacrificial mold, the ceramic substrates exhibit sufficient mechanical resistance for their handling. For further investigation, the pre-sintered substrates were divided into two groups: one for characterization and the other for the infiltration with glass to produce the desired Y-PSZ/Bioglass 45S5 composites.

Figure 6 - Sintered (white) and infiltrated (gray) 5Y-PSZ samples.

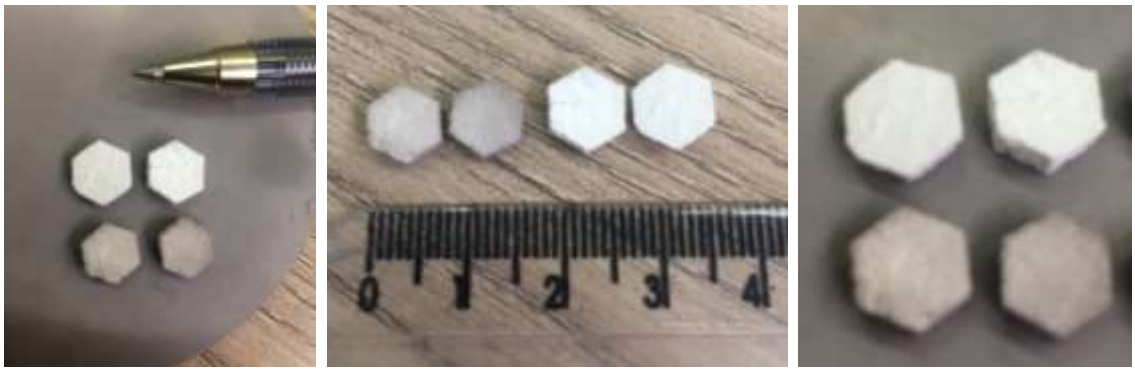

(a) (b) (c)

Source: Authors.

Figure 7 shows X-ray diffractograms of the Bioglass (a), the substrate (b), and the infiltrated substrate (c). The X-ray patterns of both, only sintered and the sintered and infiltrated substrates, are similar, showing cubic and tetragonal ZrO_2 as crystal phases, Figure 7 (b-c). The infiltration of the substrates at 1350 °C did not promote the crystallization of the Bioglass 45S5, despite literature pointing to this possibility (Prasad et. al. 2017) (Baino & Fiume, 2019). The presence of the amorphous phase may have occurred due to the slow crystallization kinetics or due to the small number of crystal phases formed, being below the detection limit of the diffractometer used. The crystal phase composition of the infiltrated samples was composed of approximately 55% of the tetragonal phase (t + t " - ZrO_2) and still 45% of the cubic phase (c -ZrO_2), forming a duplex structure of zirconia grains. Furthermore, it has also been noted that the monoclinic ZrO_2 phase, detected in the starting powder (see Figure 4) was fully converted into the cubic and tetragonal phases during the sintering/infiltration process at 1350 °C.

Figure 7 - X-ray diffractograms of a) Bioglass 45S5 powder; b) 5Y-PSZ substrate sintered at 1350 °C without infiltration and c) 5Y-PSZ substrate infiltrated with Bioglass.

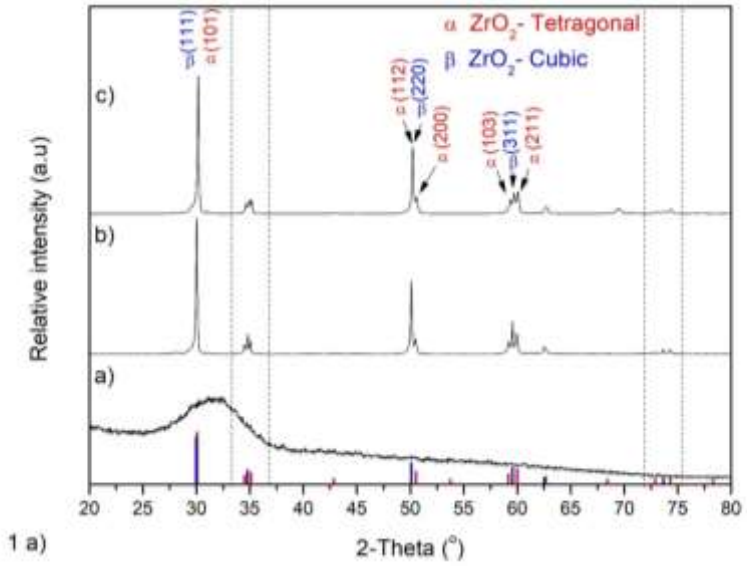

Source: Authors.

Figure 8 shows the microstructural characteristics of the zirconia substrates infiltrated with Bioglass and an EDS analysis of the element distribution.

Figure 8 - SEM micrographs of samples sintered from 5Y-PSZ and infiltrated with Bioglass 45S5: a) fracture surface; b) typical zirconia microstructure after sintering at 1350 °C-2h and c) EDS mapping of the infiltrated specimen with Bioglass.

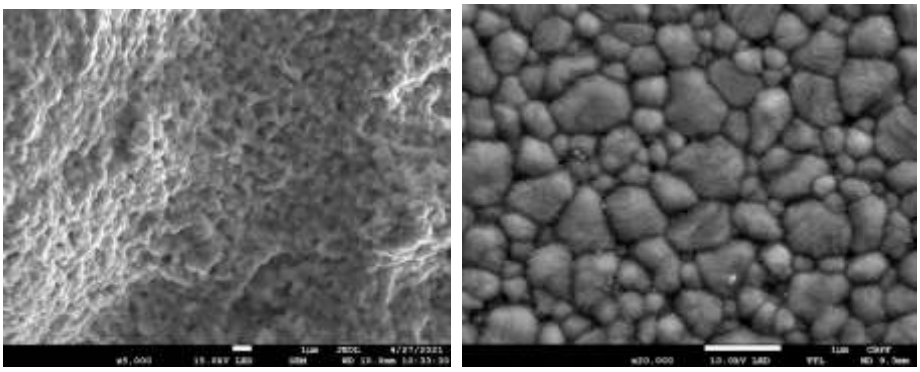

(a) (b)

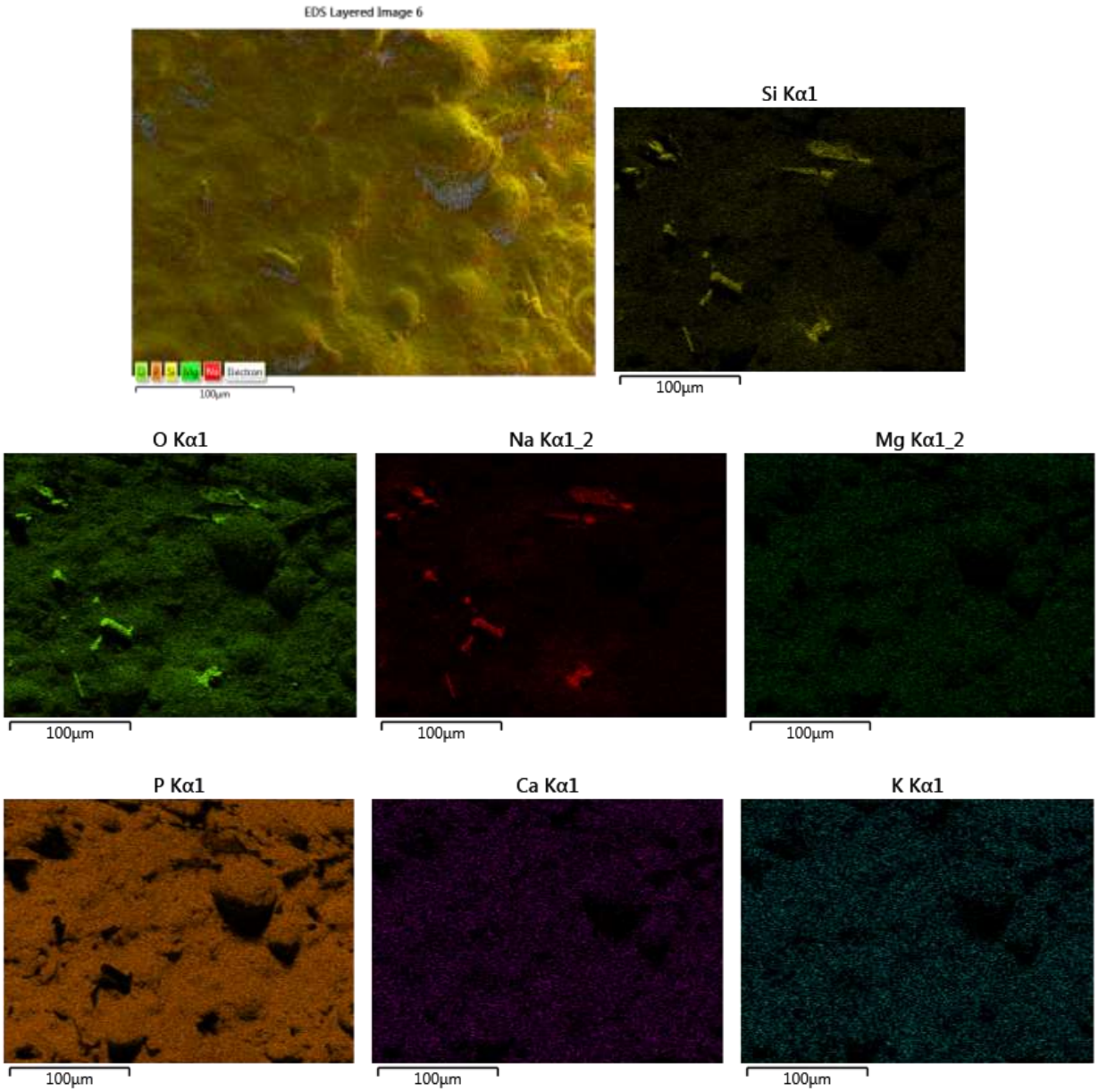

(c)

Source: Authors.

From the SEM micrographs shown in Fig. 8, it can be observed that the zirconia substrate is composed of equiaxed grains with an average size in the order of 1 µm and, from the fractured surface, an intergranular fracture mode of the matrix can be observed. Furthermore, a population of smaller grains, in the order of 0.5 - 0.7 µm corresponding to the tetragonal phase can be noted which are surrounded by grains larger than 1 µm, referring to the cubic phase, in agreement with previous results reported in the literature (Amarante et. al., 2018) (Alves et. al., 2021). This fine-grained microstructure results from the low sintering/infiltration temperature used, reducing the diffusion of Zirconia and preventing excessive grain growth. Figure 8(c) shows the EDS mapping of the zirconia substrate infiltrated Bioglass 45S5. The presence of all original constituents used in the manufacture of the Bioglass is verified and the contents analyzed are consistent with the nominal composition.

Zirconia ceramics partially stabilized with 5 mol% yttrium, 5Y-PSZ, present a significant advantage over traditional tetragonal Zirconia stabilized with 3 mol% yttria, 3Y-TZP, as they are more resistant to hydrothermal degradation in body fluids and therefore more appropriate for use as prostheses or implants. The hydrothermal degradation, which consists of the formation

of yttrium hydrides by the reaction of H_2O with Y^{3+} at the surface of the material and grain boundaries, destabilizes the tetragonal ZrO_2 phase grains, transforming them into monoclinic ZrO_2, with the result of generating microcracks at the grain boundaries, with a consequential loss of the mechanical resistance (Guo & He, 2003). However, the destabilization of the cubic (c-ZrO_2) or the pseudo-tetragonal (t " - ZrO_2) grains, or simultaneously of both (t + c), is more complex, due to the characteristics of the unit cell, the activation energy of the *t→m* transformation and due to shear stresses, resulting from the atomic organization of these phases. Therefore, the 5Y-PSZ material is more stable against hydrothermal degradation, maintaining the toughening characteristics of the tetragonal ZrO_2 grains and guaranteeing its high mechanical resistance. In the case of the 5Y-PSZ / Bioglass composite developed in this study, the vitreous phase formed by the Bioglass 45S5 must behave as a vector for the biological responses of the material, and the zirconia matrix must remain inert during its use as a biomaterial.

3.3 Mechanical properties

Table 1 presents Vickers hardness and fracture toughness of the sintered and the sintered and infiltrated substrates.

Table 1 - Properties of monolithic 5Y-PSZ ceramics sintered at 1350 °C-2h and 5Y-PSZ / Bioglass infiltrated composites.

Material	Relative density (%)	Vickers hardness (HV_{500gF})	Fracture toughness ($MPa.m^{1/2}$)
5Y-PSZ	88.5 ± 0,6	752 ± 58	2.5 ± 0,5
5Y-PSZ/Bioglass	92.3 ± 0,6	965 ± 36	4.1 ± 0,4

Source: Authors.

The monolithic zirconia substrates reached a relative density of 88.5%, reflecting the processing conditions adopted in this work. The low consolidation pressure associated with the sintering temperature of only 1350 °C-2h did not allow complete elimination of the porosity present in the pre-sintered compacts and, therefore, a residual porosity greater than 10% was observed. These characteristics are also reflected in the hardness and fracture toughness, in the order of 752 HV, and 2.5 $MPa.m^{1/2}$, inferior to about 1200 HV and 5 $MPa.m^{1/2}$ observed in similar, dense materials sintered at 1500 °C (Amarante et. al., 2018) (Alves et. al., 2021). On the other hand, the infiltration with Bioglass, leads to an increase in the relative density to more than 92% and higher hardness and fracture toughness. The glass filling the voids of the residual porosity of the substrates pre-sintered at 1200 °C improves hardness and fracture toughness. As an apparent volume of the substrate greater than 20% is occupied by the infiltrated glass, the hardness of the composite materials is less than 1200 HV, usually found in the literature. However, the fracture toughness is promising and is due to the toughening mechanisms by *t→m* of the tetragonal grain population of the material and also due to residual thermal stresses generated by the difference in the thermal expansion between Zirconia and the super-cooled glass that percolates the zirconia grains in the infiltrated material. Thus, from a structural point of view, this material has promising mechanical and physical properties for biofunctional applications; however preliminary biological tests such as *in vitro* cytotoxicity and bioactivity must be carried out to validate this composite.

4. Conclusions

Creating polymeric sacrifice molds by 3D printing allows the creation of molds of medium geometric complexity, which proved to be efficient for the manufacture of zirconia ceramic parts partially stabilized with yttria (5Y-PSZ). Substrates with a relative density of 78.5% were obtained by pre-sintering at 1200 °C. The infiltration of the porous substrates with Bioglass 45S5 was conducted at a temperature of 1350 °C-2h. During this process occurred also bulk densification (>92%), crystallization of the tetragonal and cubic ZrO_2 phases, resulting in a Vickers hardness and fracture toughness of 965 HV and 4.1 $MPa.m^{1/2}$,

respectively. These mechanical properties are sufficient for structural, biological applications. This composite is promising for biological responses of bioactivity, however specific tests have to be carried out to validate the material in cellular environments.

Acknowledgement

Dr. Claudinei dos Santos would like to thank CNPq for financial support (process 311119 / 2017-4). In addition, the authors would like to thank the CBPF (Brazilian Center for Physical Research - Laboratory of Nanostructures - LabNano) for the SEM / EDS measurements.

References

Agarwala, M. K., Jamalabad V. R., Langrana N. A., Safari. A., Whalen P. J., & Danforth, (1996), Structural quality of parts processed by fused deposition, *Rapid Prototyping Journal*, 2(4), 4-19.

Alves, M. F. R. P., Ribeiro, S., Suzuki, P. A., Strecker, K., & Santos, C. (2021) Effect of Fe_2O_3 Addition and Sintering Temperature on mechanical Properties and Translucence of Zirconia Dental Ceramics with Different Y_2O_3 Content, *Materials Research*. 24(2): e20200402

Amarante, J. E. V., Pereira, M. V. S., Souza, G. M., Alves, M. F. R. P., Simba, B. G., & Santos, C. (2018) Roughness and its effects on flexural strength of dental yttria-stabilized zirconia ceramics. Materials Science and Engineering: A., 739, 149-157.

Baino F., & Fiume, E., (2019) Elastic Mechanical Properties of 45S5-Based Bioactive Glass–Ceramic Scaffolds, *Materials*, 12, 3244.

Baino, F., Hamzehlou, S., & Kargozar, S. (2018) Bioactive glasses: Where are we and where are we going? J. Funct. Biomater., 9, 25.

Campana, V., Milano, G., Pagano, E., Barba, M., Cicione, C., Salonna, G., Lattanzi, W., & Logroscino, G. (2014) Bone substitutes in orthopaedic surgery: From basic science to clinical practice. *J. Mater. Sci. Mater. Med.*., 25, 2445–2461.

Camposilvan, E., Leone, R., Gremillard, L., Sorrentino, R., Zarone, F., Ferrari, M., & Chevalier J. (2018) Aging resistance, mechanical properties and translucency of different yttria-stabilized zirconia ceramics for monolithic dental crown applications, *Dental Materials*, 34(6) 879-890.

Daguano, J. K. M. F., Rogero, S. O., Crovace, M. C., Peitl, O., Strecker, K., & Santos, C., (2013) Bioactivity and cytotoxicity of glass and glass–ceramics based on the $3CaO{\cdot}P_2O_5$–SiO_2–MgO system, *Journal of Materials Science: Materials in Medicin*e , 24, 2171–2180.

Gibson, I., Rosen, D. W., & Stucker, B. (2010) Additive Manufacturing Technologies: Rapid Prototyping to Direct Digital Manufacturing, Springer Science+Business Media, New York, 459p.

Guo, X., & He, J. (2003), Hydrothermal degradation of cubic zirconia, *Acta Materialia*, 51 17, 5123-5130.

Hench, L. L. (1991) Bioceramics: From concept to clinic. *J. Am. Ceram. Soc.* 74, 1487–1510.

Hoppe, A., Güldal, N. S., & Boccaccini, A. R. (2011) A review of the biological response to ionic dissolution products from bioactive glasses and glass-ceramics. Biomaterials, 32, 2757–2774.

Jones, J. R., Brauer, D. S., Hupa, L., & Greenspan, D. C. (2016) Bioglass and bioactive glasses and their impact on healthcare. *Int. J. Appl. Glass Sci*., 7, 423–434.

Juraski, A. C., Figueiredo, D. C., Daghastanli N. A., Santos, C., Fernandes, M. H. V., da Ana, P. A., & Daguano J. K. M. B. (2021) Effect of a whitlockite glass-ceramic on the occlusion of dentinal tubules for dentin hypersensitivity treatment, Research, Society and Development, 10 (3), e19610313161

Karakurt I., & Lin, L., (2020) 3D printing technologies: techniques, materials, and post-processing, *Current Opinion in Chemical Engineering*, 28, 134-143

Kim, H. S., Kumbar, S. G., & Nukavarapu, S. P. (2021), Review: Biomaterial-directed cell behavior for tissue engineering, Current Opinion in biomedical engineering, 17, 100260

Rahaman, M. N., Day, D. E., Bal, B. S., Fu, Q., Jung, S. B., Bonewald, L. F., & Tomsia, A. P. (2011) Bioactive glass in tissue engineering. Acta Biomater., 7, 2355–2373.

Prasad, S., Vyas, V. K., Ershad, M. D., & Pyare, R. (2017) Crystallization and mechanical properties of (45S5-HA) biocomposite for implantation , *Ceramics-Silikáty* 61 (4), 378-384

Reveron, H., & Chevalier, J. (2021), Yttria-stabilized zirconia as a biomaterial: from orthopedic towards dental applications, *Encyclopedia os materials technical ceramics and glasses*, 3, 540-552.

Zhou M. Y., Xi, J. T., & Yan, J. Q. (2004) Adaptive direct slicing with non-uniform cusp heights for rapid prototyping. Int J Adv Manuf Technol 23(1–2):20–27.